IRF9 Prevents CD8+ T Cell Exhaustion in an Extrinsic Manner during Acute Lymphocytic Choriomeningitis Virus Infection

Magdalena Huber,[a] Tamara Suprunenko,[b] Thomas Ashhurst,[c] Felix Marbach,[a] Hartmann Raifer,[a] Svenja Wolff,[d] Thomas Strecker,[d] Barney Viengkhou,[b] So Ri Jung,[b] Hannah-Lena Obermann,[e] Stefan Bauer,[e] Haifeng C. Xu,[f] Philipp A. Lang,[f] Adomati Tom,[g] Karl S. Lang,[g] Nicholas J. C. King,[c] Iain L. Campbell,[h] Markus J. Hofer[b,i]

Institute of Medical Microbiology and Hygiene, University of Marburg, Marburg, Germany[a]; School of Life and Environmental Sciences, the Marie Bashir Institute for Infectious Diseases and Biosecurity, the Charles Perkins Centre, and the Bosch Institute, The University of Sydney, Sydney, Australia[b]; Department of Pathology and the Bosch Institute, School of Medical Sciences, Sydney Medical School, University of Sydney, Sydney, Australia, and Sydney Cytometry Facility, The University of Sydney and the Centenary Institute, Sydney, Australia[c]; Institute of Virology, University of Marburg, Marburg, Germany[d]; Institute of Immunology, University of Marburg, Marburg, Germany[e]; Institute of Molecular Medicine II, University of Düsseldorf, Düsseldorf, Germany[f]; Institute of Immunology, University Hospital Essen, Essen, Germany[g]; School of Molecular Bioscience, the Marie Bashir Institute for Infectious Diseases and Biosecurity, the Charles Perkins Centre, and the Bosch Institute, The University of Sydney, Sydney, Australia[h]; Department of Neuropathology, University of Marburg, Marburg, Germany[i]

ABSTRACT Effective CD8+ T cell responses play an important role in determining the course of a viral infection. Overwhelming antigen exposure can result in suboptimal CD8+ T cell responses, leading to chronic infection. This altered CD8+ T cell differentiation state, termed exhaustion, is characterized by reduced effector function, upregulation of inhibitory receptors, and altered expression of transcription factors. Prevention of overwhelming antigen exposure to limit CD8+ T cell exhaustion is of significant interest for the control of chronic infection. The transcription factor interferon regulatory factor 9 (IRF9) is a component of type I interferon (IFN-I) signaling downstream of the IFN-I receptor (IFNAR). Using acute infection of mice with lymphocytic choriomeningitis virus (LCMV) strain Armstrong, we show here that IRF9 limited early LCMV replication by regulating expression of interferon-stimulated genes and IFN-I and by controlling levels of IRF7, a transcription factor essential for IFN-I production. Infection of IRF9- or IFNAR-deficient mice led to a loss of early restriction of viral replication and impaired antiviral responses in dendritic cells, resulting in CD8+ T cell exhaustion and chronic infection. Differences in the antiviral activities of IRF9- and IFNAR-deficient mice and dendritic cells provided further evidence of IRF9-independent IFN-I signaling. Thus, our findings illustrate a CD8+ T cell-extrinsic function for IRF9, as a signaling factor downstream of IFNAR, in preventing overwhelming antigen exposure resulting in CD8+ T cell exhaustion and, ultimately, chronic infection.

IMPORTANCE During early viral infection, overwhelming antigen exposure can cause functional exhaustion of CD8+ T cells and lead to chronic infection. Here we show that the transcription factor interferon regulatory factor 9 (IRF9) plays a decisive role in preventing CD8+ T cell exhaustion. Using acute infection of mice with LCMV strain Armstrong, we found that IRF9 limited early LCMV replication by regulating expression of interferon-stimulated genes and *Irf7*, encoding a transcription factor crucial for type I interferon (IFN-I) production, as well as by controlling the

levels of IFN-I. Infection of IRF9-deficient mice led to a chronic infection that was accompanied by CD8+ T cell exhaustion due to defects extrinsic to T cells. Our findings illustrate an essential role for IRF9, as a mediator downstream of IFNAR, in preventing overwhelming antigen exposure causing CD8+ T cell exhaustion and leading to chronic viral infection.

KEYWORDS CD8+ T cell exhaustion, interferon regulatory factor 9, lymphocytic choriomeningitis virus, type I interferon

During viral infection, the host immune response must strike a delicate balance between effectively eliminating the virus and preventing tissue damage. Cytotoxic CD8+ T cells are a key component of this adaptive antiviral response. Acute infection triggers the generation of short-lived effector cells (SLECs) and long-lived memory CD8+ T cells. Effector CD8+ T cells have high cytotoxic activity and coexpress multiple cytokines, including gamma interferon (IFN-γ) and tumor necrosis factor alpha (TNF-α) (1). However, in chronic infection, uncontrolled viral replication results in high antigen exposure. When antigen exposure becomes overwhelming, differentiation of CD8+ T cells moves toward a dysfunctional pathway termed functional exhaustion. This CD8+ T cell state is reversible and is associated with the expression of inhibitory receptors, including programmed cell death 1 (PD1) and lymphocyte activation gene 3 (LAG3) (2, 3). Exhausted CD8+ T cells are characterized by impaired proliferation and effector cytokine production. However, they retain some effector function, allowing them to restrict ongoing viral replication while preventing tissue damage (4, 5).

Type I interferons (IFN-I), including IFN-α and IFN-β, are cytokines with essential antiviral functions during early infection (6, 7). They assist in the activation and differentiation of CD8+ T cells, thus enhancing the CD8+ T cell-mediated antiviral immune response (3). IFN-I bind to and signal through a heterodimeric receptor composed of two subunits, IFNAR1 and IFNAR2. The ligation of IFNAR activates several signal transduction pathways, including STAT1 homodimers, STAT3 homodimers, the mitogen-activated protein kinase (MAPK) pathway, phosphatidylinositol 3-kinase (PI3K)–AKT, and IFN-stimulated gene factor 3 (ISGF3), consisting of STAT1-STAT2 heterodimers and the transcription factor (TF) interferon regulatory factor 9 (IRF9) (6, 7). It is not clear how each of these pathways contributes to the outcome of a viral infection. In the present study, we focused on IRF9, which is present at steady-state levels in most human and murine cell types and is strongly upregulated in an autocrine loop by IFN-I signaling (8). So far, IRF9-mediated induction of IFN-I and antiviral effector gene expression has been demonstrated in mouse embryonic fibroblasts (EFs) and mutant cell lines (9–13). Furthermore, studies with EFs and human tumor cell lines (14, 15) have shown that IRF9 is required for expression of the gene for the TF IRF7, which is a crucial mediator and amplifier of IFN-I production in plasmacytoid dendritic cells (pDCs) (16, 17). In addition, we previously showed that in contrast to STAT1-deficient mice, which develop a lethal wasting disease following infection with lymphocytic choriomeningitis virus (LCMV), mice lacking IRF9 survive (18). However, the molecular mechanisms underlying these major differences in the outcome of infection in STAT1- versus IRF9-deficient mice remain unclear. In particular, the contributions of IRF9 to the innate and adaptive antiviral immune responses and its role in the activation of DCs, including *Irf7* expression, are still unknown.

Here we analyzed the impact of IRF9 on the antiviral immune response during infection with the prototypic Armstrong strain of LCMV (LCMV-Arm). LCMV-Arm typically causes acute infection in mice. In the absence of IRF9, infection became chronic and was characterized by CD8+ T cell exhaustion and impaired expression of the *Irf7* gene and antiviral effector molecules. This suggests that IRF9 is an essential factor downstream of IFNAR for early viral control, thus preventing CD8+ T cell exhaustion in an extrinsic manner and, as a consequence, viral persistence.
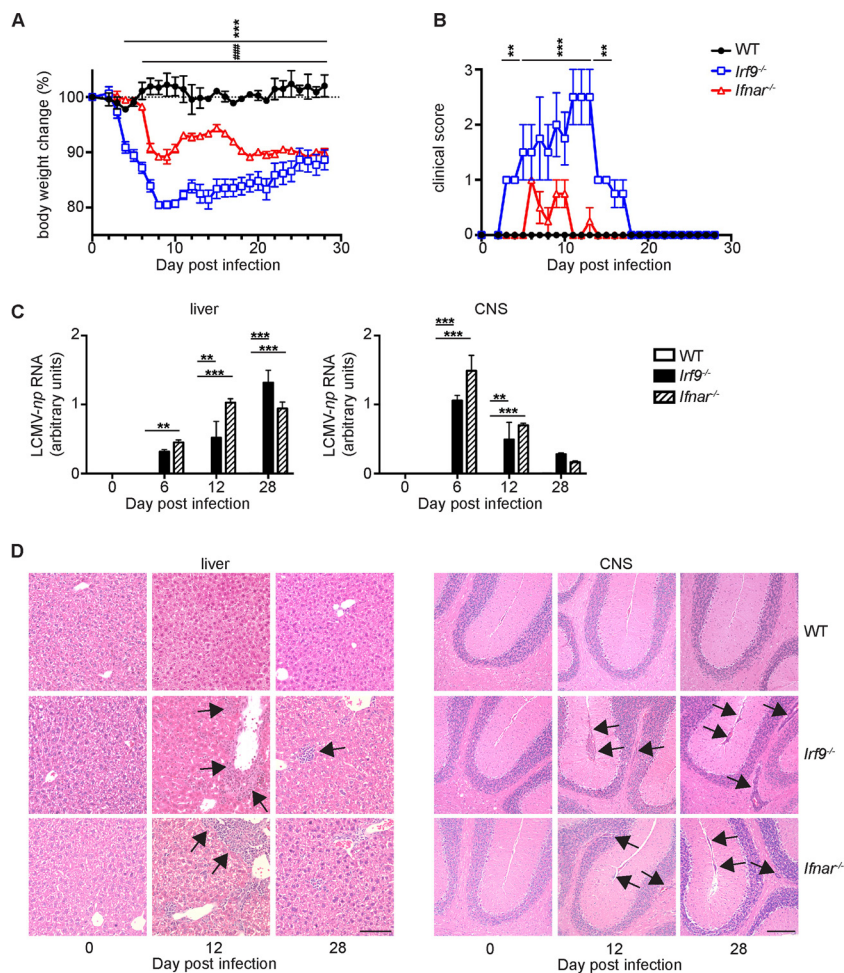
FIG 1 IRF9 deficiency converts acute LCMV-Arm infection into a chronic infection associated with inflammatory changes. (A to D) WT, Irf9$^{-/-}$, and Ifnar$^{-/-}$ mice were infected with LCMV-Arm i.p. and analyzed at the indicated time points p.i. Weight curves (A) and clinical scores (B) for infected mice are shown. (C) LCMV-np RNA levels in livers and CNS of WT, Irf9$^{-/-}$, and Ifnar$^{-/-}$ mice. The LCMV-np RNA levels were normalized to Rpl32 mRNA levels. Data are means and standard errors of the means (SEM). (D) Histological changes in hematoxylin and eosin (H&E)-stained sections of WT, Irf9$^{-/-}$, and Ifnar$^{-/-}$ mice. Arrows point to inflammatory infiltrates in livers and CNS of infected Irf9$^{-/-}$ and Ifnar$^{-/-}$ mice. Bars = 100 μm. For all panels, experiments were repeated three times with consistent results. Asterisks indicate comparisons of WT versus Irf9$^{-/-}$ mice, and number (#) symbols indicate comparison of WT versus Ifnar$^{-/-}$ mice. *, $P < 0.05$; **, $P < 0.01$; ***, $P < 0.001$. One-way analysis of variance (ANOVA) with Tukey's posttest was used for multiple comparisons.

RESULTS

Irf9$^{-/-}$ mice fail to clear LCMV and develop chronic inflammation. To analyze the role of IRF9 during antiviral immune responses, we infected wild-type (WT), IFNAR-deficient (Ifnar$^{-/-}$), and IRF9-deficient (Irf9$^{-/-}$) mice with LCMV-Arm. LCMV-Arm evokes a strong CD8$^+$ T cell response, which controls viral replication and clears infection within approximately 12 days in WT mice (19, 20). In contrast, the CD8$^+$ T cell response is severely impaired in Ifnar$^{-/-}$ mice, and LCMV persists for a prolonged time (21). As expected, upon intraperitoneal (i.p.) infection, WT mice developed a slight and transient weight loss and cleared the virus, resulting in undetectable viral RNA in analyzed organs by day 12 postinfection (p.i.) (Fig. 1A to C). Following infection, Irf9$^{-/-}$ mice also developed a transient disease. However, they had more severe signs of disease than WT or Ifnar$^{-/-}$ mice, with more significant weight loss (Fig. 1A) and clinical signs, including rough fur and hunched posture (Fig. 1B). In both Irf9$^{-/-}$ and Ifnar$^{-/-}$ mice, LCMV replication was not controlled and the virus persisted (Fig. 1C). This was accompanied by marked infiltration of the liver and the central nervous system (CNS)

with leukocytes (Fig. 1D). These results suggest that IRF9 contributes to LCMV-Arm clearance by affecting CD8$^+$ T cell responses.

IRF9 deficiency results in exhaustion of LCMV-specific CD8$^+$ T cells. To understand the impact of IRF9 on the antigen-specific CD8$^+$ T cell response, we performed dextramer staining for CD8$^+$ T cells specific for LCMV glycoprotein (GP) and nucleoprotein (NP). Consistent with the clinical data, in $Irf9^{-/-}$ mice, accumulation of virus-specific CD8$^+$ T cells was strongly reduced compared to that in WT mice (Fig. 2A). Further, the total number of GP$_{33-41}$- and NP$_{396-404}$-specific CD8$^+$ T cells was comparably reduced in $Irf9^{-/-}$ and $Ifnar^{-/-}$ mice (Fig. 2A). Upon antigen recognition, activated CD8$^+$ T cells upregulate CD44 and SLECs display the molecule killer cell lectin-like receptor G1 (KLRG1) (1). Interestingly, virus-specific CD8$^+$ T cells from WT, $Ifnar^{-/-}$, and $Irf9^{-/-}$ mice had similar CD44 levels (Fig. 2B), suggesting that CD8$^+$ T cells in all three mouse strains were activated by LCMV. WT CD8$^+$ T cells displayed high levels of KLRG1, suggesting that differentiation into SLECs is important for containment of infection. In contrast, KLRG1 expression on virus-specific CD8$^+$ T cells from infected $Irf9^{-/-}$ and $Ifnar^{-/-}$ mice was strongly reduced (Fig. 2C). Functionally, SLECs are characterized by the production of multiple cytokines, including IFN-γ and TNF-α (1). Virus-specific production of IFN-γ and TNF-α was high in WT CD8$^+$ T cells (Fig. 2D). This was consistent with high KLRG1 expression and clearance of infection. In contrast, CD8$^+$ T cells from infected $Irf9^{-/-}$ and $Ifnar^{-/-}$ mice displayed significantly reduced production of these effector cytokines in response to viral peptide (Fig. 2D), in agreement with the diminished expression of KLRG1 (Fig. 2C). Thus, virus-specific CD8$^+$ T cells from LCMV-infected $Irf9^{-/-}$ and $Ifnar^{-/-}$ mice showed impaired accumulation and function as assessed by production of effector cytokines. Combining these results with LCMV-Arm persistence (Fig. 1), we hypothesized that this impairment was due to functional exhaustion of CD8$^+$ T cells. In line with our hypothesis, we detected increased levels of the inhibitory receptors PD1 and LAG3 on virus-specific CD8$^+$ T cells after LCMV infection of $Irf9^{-/-}$ mice (Fig. 2E and F). While CD8$^+$ T cells from $Ifnar^{-/-}$ mice had similarly increased PD1 levels, LAG3 levels were even higher in $Ifnar^{-/-}$ mice than in $Irf9^{-/-}$ mice, indicating differential regulation of the expression of the two inhibitory receptor genes by IFNAR and IRF9 signaling. Thus, infection with LCMV-Arm causes CD8$^+$ T cell exhaustion in $Irf9^{-/-}$ and $Ifnar^{-/-}$ mice.

T cell-extrinsic IRF9 deficiency causes CD8$^+$ T cell exhaustion upon LCMV-Arm infection. To understand whether CD8$^+$ T cell exhaustion in LCMV-Arm-infected $Irf9^{-/-}$ and $Ifnar^{-/-}$ mice is caused by CD8$^+$ T cell-extrinsic functions of IRF9 and IFNAR, respectively, we adoptively transferred CD8$^+$ T cells from a mouse with a transgenic T cell receptor (P14) recognizing the LCMV peptide GP$_{33-41}$ (22) into WT, $Irf9^{-/-}$, or $Ifnar^{-/-}$ mice. As expected, the transfer of P14 cells into WT mice followed by LCMV-Arm infection caused an accumulation of virus-specific CD8$^+$ T cells with the SLEC phenotype as characterized by high KLRG1 levels and strong production of IFN-γ and TNF-α (Fig. 3A to F). Conversely, in an $Irf9^{-/-}$ environment, P14 cells accumulated less and failed to acquire the effector phenotype as assessed by impaired KLRG1 expression and reduced production of IFN-γ and TNF-α (Fig. 3A, C, and E). The findings were similar for $Ifnar^{-/-}$ recipient mice (Fig. 3B, D, and F). Consistent with reduced KLRG1 expression and cytokine production, P14 cells transferred into $Irf9^{-/-}$ or $Ifnar^{-/-}$ mice displayed increased PD1 and LAG3 levels (Fig. 4A to D), indicating their functional exhaustion. This was accompanied by imbalanced levels of the TFs T-bet and Eomes (Fig. 4E to H), as described for exhausted CD8$^+$ T cells (2). Surprisingly, the transfer of $Irf9^{-/-}$ P14 cells into WT mice failed to upregulate markers of exhaustion on virus-specific P14 cells (Fig. 4I and J). These results reveal that IRF9 and IFNAR prevent CD8$^+$ T cell exhaustion upon LCMV-Arm infection in a manner extrinsic to CD8$^+$ T cells.

IRF9 is critical for IFN-I production and expression of ISGs and IRF7 in DCs. As professional antigen-sensing and -presenting cells, DCs are crucial for the appropriate induction of T cell activation. Previous studies have shown that priming of CD8$^+$ T cells by LCMV is dependent on DCs (23–25) and that defects in DC function can lead to T cell
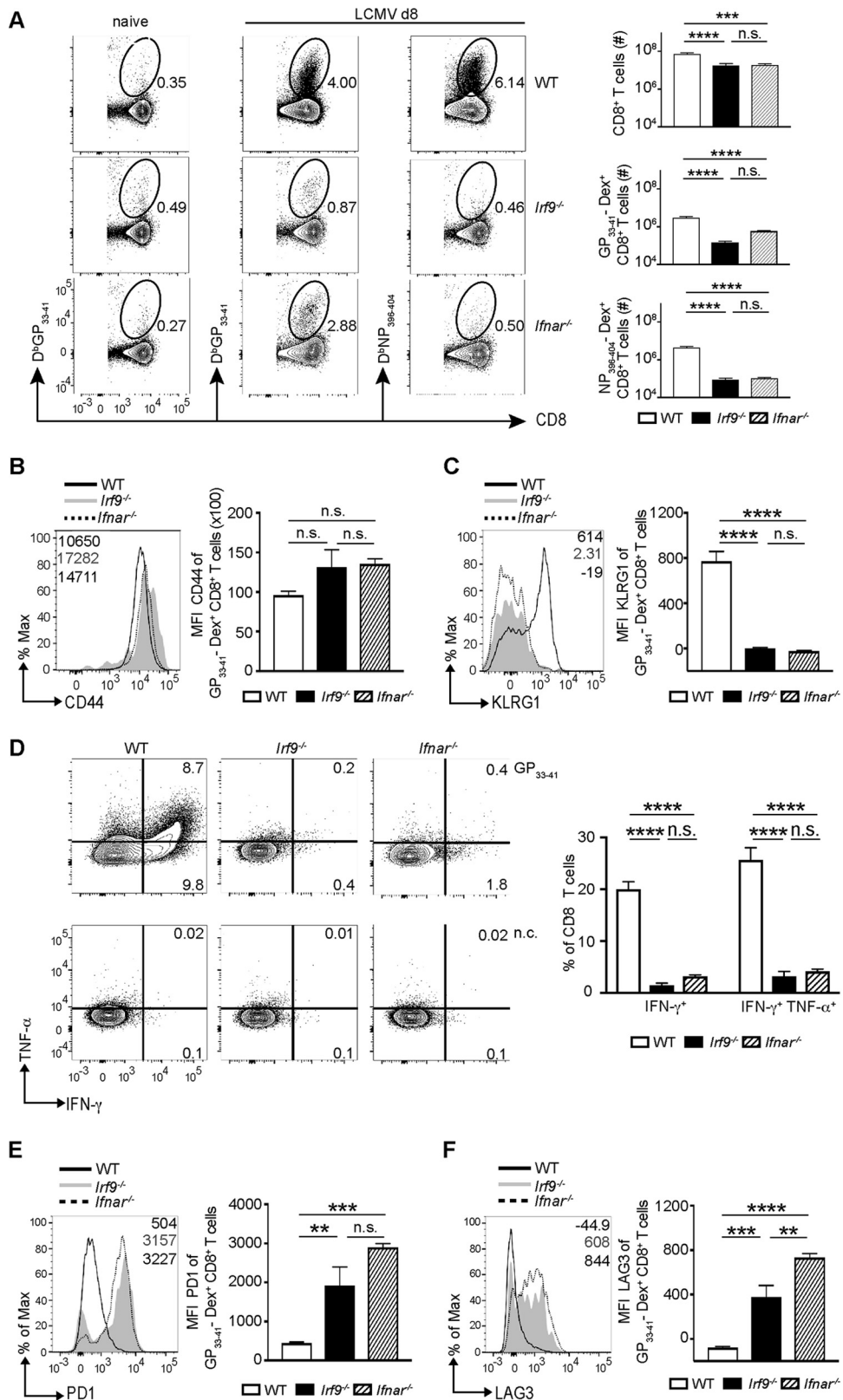
FIG 2 IRF9 deficiency impairs accumulation of effector CD8$^+$ T cells and induces exhaustion. (A to F) WT, $Irf9^{-/-}$, and $Ifnar^{-/-}$ mice were infected with LCMV-Arm i.p., and the spleens were analyzed at day 8 p.i. (A) Frequencies of CD8$^+$ T cells and LCMV GP$_{33-41}$ and LCMV NP$_{396-404}$ dextramer-positive (Dex$^+$) CD8$^+$ T cells in WT, $Irf9^{-/-}$, and $Ifnar^{-/-}$ mice. Left panels depict GP$_{33-41}$ Dex$^+$ CD8$^+$ T cells in naive (uninfected) mice. (B and C) Mean fluorescence intensities (MFI) for CD44 and KLRG1 of LCMV-GP$_{33-41}$ Dex$^+$ CD8$^+$ T cells in WT, $Irf9^{-/-}$, and $Ifnar^{-/-}$ mice.
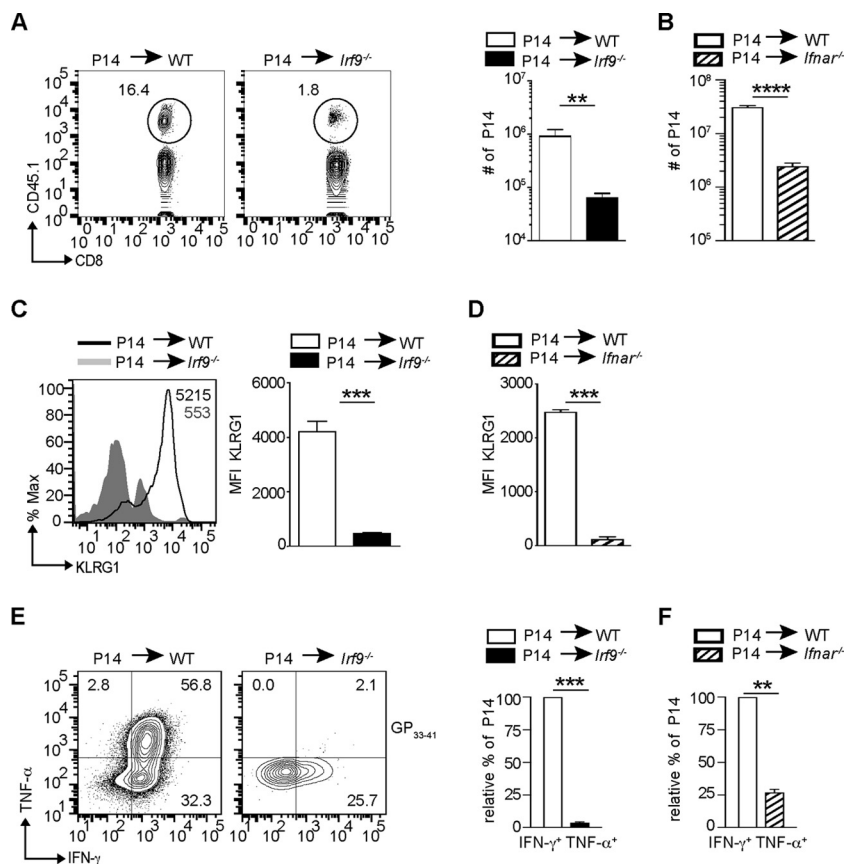
(Continued on next page)

FIG 3 IRF9 extrinsically regulates the accumulation of effector CD8$^+$ T cells. (A to F) Prior to LCMV-Arm infection, 10^4 negatively sorted CD8$^+$ T cells from CD45.1$^+$ P14 mouse cells were transferred into WT or $Irf9^{-/-}$ mice (A, C, and E) or into WT or $Ifnar^{-/-}$ mice (B, D, and F). The spleens were analyzed at day 8 p.i. (A) Representative contour plots give CD45.1 and CD8α staining of transferred P14 cells in WT and $Irf9^{-/-}$ mice. The numbers show percentages of positive cells. The bar diagram to the right shows the number of P14 cells among total splenocytes. (B) Number of P14 cells among total splenocytes in WT or $Ifnar^{-/-}$ recipients. (C) MFI for KLRG1 of P14 cells transferred into WT or $Irf9^{-/-}$ mice. Representative histograms and bar diagrams are shown. (D) MFI for KLRG1 of P14 cells transferred into WT or $Ifnar^{-/-}$ recipients. (E) Splenocytes were stimulated with GP$_{33-41}$ peptide and analyzed for intracellular IFN-γ and TNF-α production. The left panels display representative contour plots, in which the numbers indicate percentages of positive cells. The bar diagram to the right gives percentages of P14 cells, with the WT level set to 100%. (F) Percentage of IFN-γ^+ TNF-α^+ P14 cells transferred into WT or $Ifnar^{-/-}$ recipients. All bar diagrams show means and SEM ($n = 5$ mice per group). Data from one of two independent experiments with consistent results are shown. *, $P < 0.05$; **, $P < 0.01$; ***, $P < 0.001$ (unpaired two-tailed Student's t test).

exhaustion (2). Also, DCs are one of the primary targets of LCMV, as they express the virus receptor α-dystroglycan (α-DG) at high levels (24, 26). Since CD8$^+$ T cell exhaustion in $Irf9^{-/-}$ and $Ifnar^{-/-}$ mice was caused by effects extrinsic to T cells, we hypothesized that IRF9-dependent IFN-I signaling is critical for the function of DCs. Cell cultures containing all subpopulations of DCs, including a significant fraction of pDCs, can be generated from murine bone marrow (BM) by use of FMS-like tyrosine kinase 3 ligand (Flt3L) (27). Thus, we next analyzed Flt3L-derived DCs (Flt3L-DCs) from WT and $Irf9^{-/-}$ mice for the ability to produce IFN-I following addition of RNA40, which triggers

FIG 2 Legend (Continued)

(D) Splenocytes were stimulated with GP$_{33-41}$ peptide and analyzed for IFN-γ and TNF-α production by intracellular staining. n.c., nonstimulated control. The numbers display percentages of positive cells. (E and F) MFI for PD1 and LAG3 of LCMV-GP$_{33-41}$ Dex$^+$ CD8$^+$ T cells in WT, $Irf9^{-/-}$, and $Ifnar^{-/-}$ mice. For all panels, representative histograms are shown, and bar diagrams display means and SEM ($n = 5$ per group). Data from one of two independent experiments with consistent results are shown. **, $P < 0.01$; ***, $P < 0.001$; ****, $P < 0.0001$; n.s., not significant (unpaired two-tailed Student's t test).
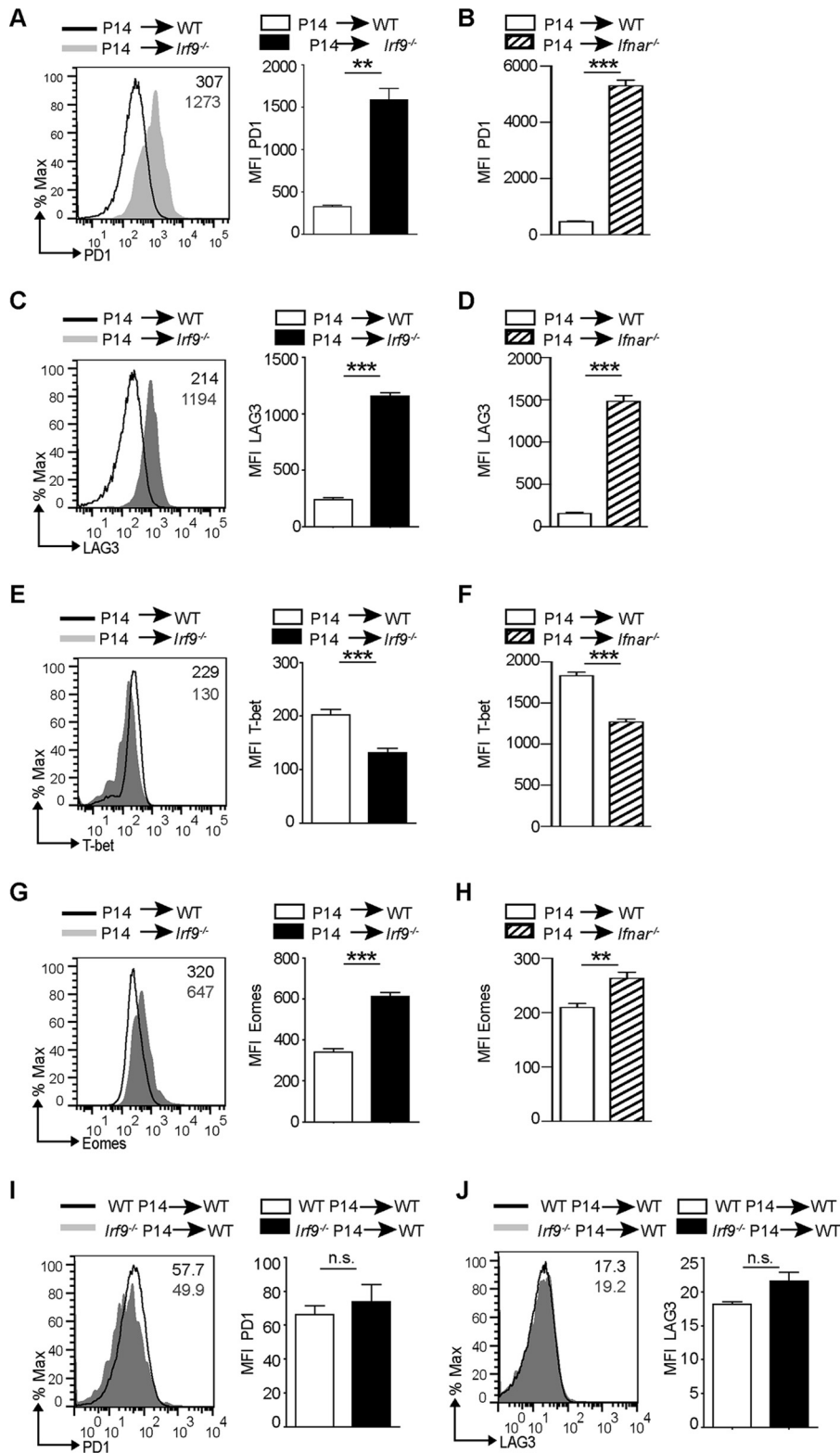
FIG 4 IRF9 extrinsically regulates exhaustion of CD8+ T cells. Prior to LCMV-Arm infection, 10⁴ negatively sorted CD8+ T cells from CD45.1+ P14 mouse cells were transferred into WT or *Irf9⁻/⁻* mice (A, C, E, and G) or into WT or *Ifnar⁻/⁻* mice (B, D, F, and H). Spleens were analyzed at day 8 p.i. (A to H) MFI for LAG3, PD1, Eomes, and T-bet of P14 cells transferred into WT, *Irf9⁻/⁻*, or *Ifnar⁻/⁻* mice. Representative histograms are shown. Bar diagrams display means and SEM (*n* = 5 per group). (I and J) Prior to LCMV-Arm infection, 10⁴ negatively sorted CD8+ T cells from CD45.2+ P14 mice or from CD45.2+ *Irf9⁻/⁻* P14 mice were transferred into CD45.1+ WT mice. The spleens were analyzed at day 8 p.i., and the graphs show MFI for
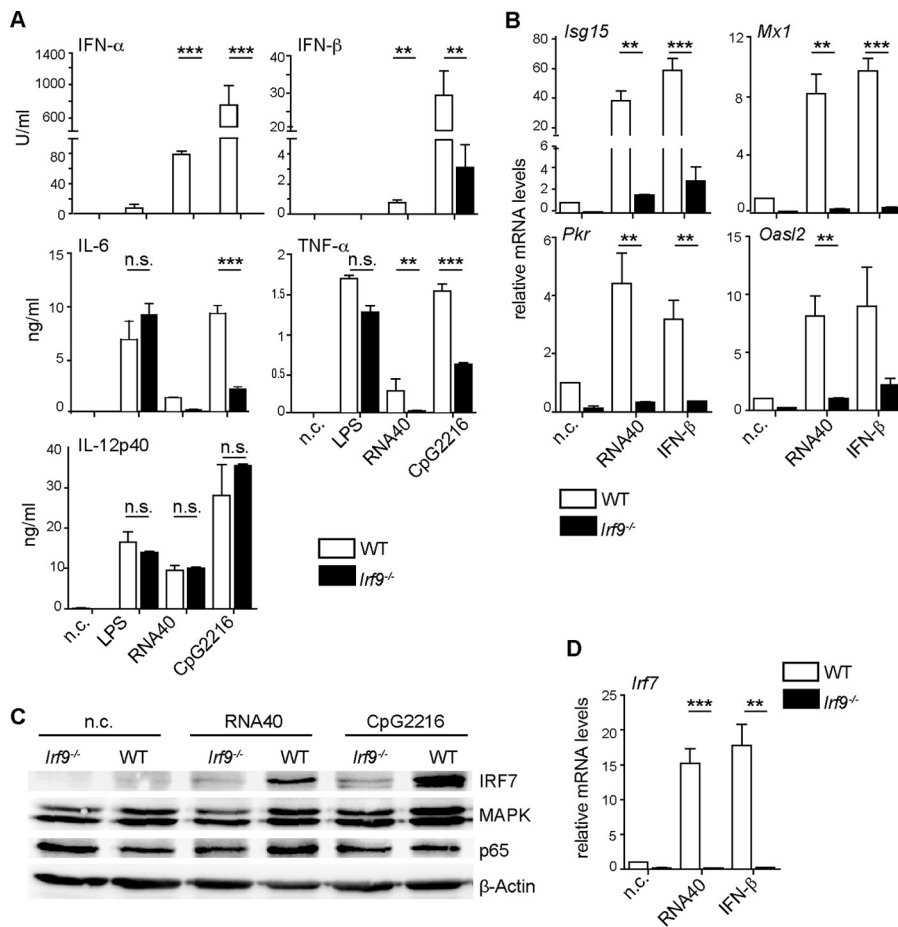
FIG 5 IRF9 is important for DC function in response to IFN-I and TLR7 as well as TLR9 ligands. (A to D) WT or $Irf9^{-/-}$ Flt3L-DCs were left unstimulated (n.c.) or were stimulated with LPS, RNA40 complexed to DOTAP, CpG2216, or IFN-β. (A) Cytokine concentrations were measured by ELISA after 22 h of stimulation. (B and D) mRNA levels for the indicated genes were analyzed by qRT-PCR analysis and normalized to the levels of *Hprt1*. Relative expression was calculated by setting the value for unstimulated WT Flt3L-DCs to 1. (C) Immunoblotting of IRF7, MAPK, p65, and β-actin in WT or $Irf9^{-/-}$ Flt3L-DCs after 22 h of stimulation with RNA40 or CpG2216 or in unstimulated cells (n.c.). For panel A, data were combined from three independent experiments performed in duplicate and are means and SEM. For panels B and D, data were combined from two independent experiments performed in duplicate and are means and SEM. For panel C, data from one of three independent experiments with consistent results are shown. **, $P < 0.01$; ***, $P < 0.001$; n.s., not significant (Student's t test).

Toll-like receptor 7 (TLR7) activation (imitating the single-stranded RNA displayed by LCMV), or CpG oligodeoxynucleotides (ODNs), which induce TLR9 signaling. We found that Flt3L-DCs from $Irf9^{-/-}$ mice produced less IFN-I and proinflammatory cytokines interleukin-6 (IL-6) and TNF-α in response to the TLR7 and TLR9 agonists, while the production of IL-12p40 was not significantly affected (Fig. 5A). Because IFN-I are known to upregulate IL-6 and TNF-α production, it is possible that the diminished production upon RNA40 and CpG ODN stimulation resulted from the deficiency in IFN-I production (28). Furthermore, the production of IL-6 and TNF-α in response to the TLR4 agonist lipopolysaccharide (LPS) was not affected by IRF9 deficiency in Flt3L-DCs, suggesting that the contribution of IRF9 to TLR responses is specific for TLR7 and TLR9. IFN-

FIG 4 Legend (Continued)

PD1 and LAG3 of WT or $Irf9^{-/-}$ P14 cells transferred into WT mice. Representative histograms are shown. Bar diagrams to the right display means and SEM ($n = 5$ per group). For panels A to F, data from one of two independent experiments with consistent results are shown. **, $P < 0.01$; ***, $P < 0.001$; n.s., not significant (unpaired two-tailed Student's t test).

inducible antiviral effectors are critical for the early inhibition of viral replication (29). Given the impaired control of LCMV in $Irf9^{-/-}$ mice, we therefore analyzed the regulation of virus-restricting IFN-stimulated gene (ISG) expression by IRF9 in DCs. We observed strongly reduced expression of antiviral effectors upon TLR7 stimulation or IFN-β addition in IRF9-deficient versus WT Flt3L-DCs (Fig. 5B).

Signal transduction via TLR7 and TLR9 involves several signaling pathways, including NF-κB, MAPK, and IRF7 pathways. In particular, IRF7 is required for the IFN-I response in pDCs (16, 17). We found that IRF9 was required for IRF7 upregulation in Flt3L-DCs, whereas the p65 subunit of the classical NF-κB pathway, as well as MAPK, was not strongly affected by IRF9 deficiency (Fig. 5C). This regulation occurred at the level of gene expression, as $Irf7$ expression was strongly diminished in $Irf9^{-/-}$ versus WT Flt3L-DCs (Fig. 5D). Thus, IRF9 contributes to the upregulation of IFN-I and IRF7 upon TLR7 and TLR9 signaling and to the induction of antiviral ISGs in Flt3L-DCs.

IRF9 is required for normal DC activation *in vivo* and for early control of LCMV replication. To understand the contribution of IRF9 to the control of LCMV infection, we analyzed plasma levels of IFN-I in $Irf9^{-/-}$ versus WT mice upon LCMV infection. We noted significantly diminished IFN-α levels, while IFN-β was less affected by IRF9 deficiency (Fig. 6A). The main producers of IFN-I during early viral infection are pDCs, and this function is tightly controlled by IRF7 (16, 17). Therefore, we investigated whether IRF9 affects the functional qualities of pDCs during LCMV infection in comparison to those seen with IFNAR. For this purpose, we purified pDCs 1 day after LCMV infection and analyzed the expression of key genes by quantitative real-time PCR (qRT-PCR). Consistent with our *in vitro* data, *ex vivo*-enriched pDCs from day 1 infected $Irf9^{-/-}$ mice displayed strongly diminished $Irf7$ gene expression compared to that in pDCs from WT mice (Fig. 6B). Furthermore, the expression of antiviral effector genes by pDCs was markedly decreased by IRF9 deficiency (Fig. 6C). This was accompanied by loss of control of early LCMV replication in DCs and metallophilic macrophages in spleens of $Irf9^{-/-}$ mice (Fig. 6D and E). Notably, while mRNA levels for $Irf7$, $Isg15$, Pkr, $Oasl2$, and $Mx1$ were reduced in IRF9-deficient pDCs compared to those in WT cells, they were even lower in pDCs from $Ifnar^{-/-}$ mice (Fig. 6B and C), indicating that in the absence of IRF9 a partial signaling via IFNAR takes place. However, this partial signaling is not sufficient for restriction of viral replication and prevention of T cell exhaustion. In agreement with partial IFNAR signaling being present with IRF9 deficiency, levels of the IFN-inducible activation marker stem cell antigen 1 (SCA-1) (30) in $Irf9^{-/-}$ pDCs and conventional DCs (cDCs) were between those in WT and $Ifnar^{-/-}$ mice (Fig. 6F). In addition, we detected a differentially imbalanced expression of the costimulatory molecules CD80 and CD86 on pDCs and cDCs from $Irf9^{-/-}$ and $Ifnar^{-/-}$ mice (Fig. 6G and H), suggesting that IRF9 and IFN-I may also affect the costimulatory activity of pDCs and cDCs, and thus the priming of CD8$^+$ T cells (31), in a noncompletely overlapping manner. Taken together, these data demonstrate a crucial role for IRF9 as a signaling factor downstream of IFNAR in the early control of LCMV infection, by upregulating IFN-I production, as well as in the expression of antiviral effector genes. These effects combined with modulation of the properties of DCs by IRF9 determine adequate CD8$^+$ T cell responses in the control of LCMV dissemination.

DISCUSSION

In this study, we demonstrated that the transcription factor IRF9 is critical for the early control of LCMV-Arm infection and its subsequent elimination. We also showed that IRF9 is the crucial mediator downstream of IFNAR in the antiviral IFN-I response. The absence of IRF9 converted acute LCMV-Arm infection into a chronic infection associated with functional CD8$^+$ T cell exhaustion. IRF9 was critical for the upregulation of antiviral effectors *in vitro* in Flt3L-DCs in response to the TLR7 agonist RNA40 or IFN-I. Similarly, upon LCMV-Arm infection of $Irf9^{-/-}$ mice, the expression of antiviral effectors in pDCs, including $Mx1$ and Pkr, as well as SCA-1 in DC subsets, was strongly impaired, with evident loss of early restriction of LCMV replication. This demonstrates that
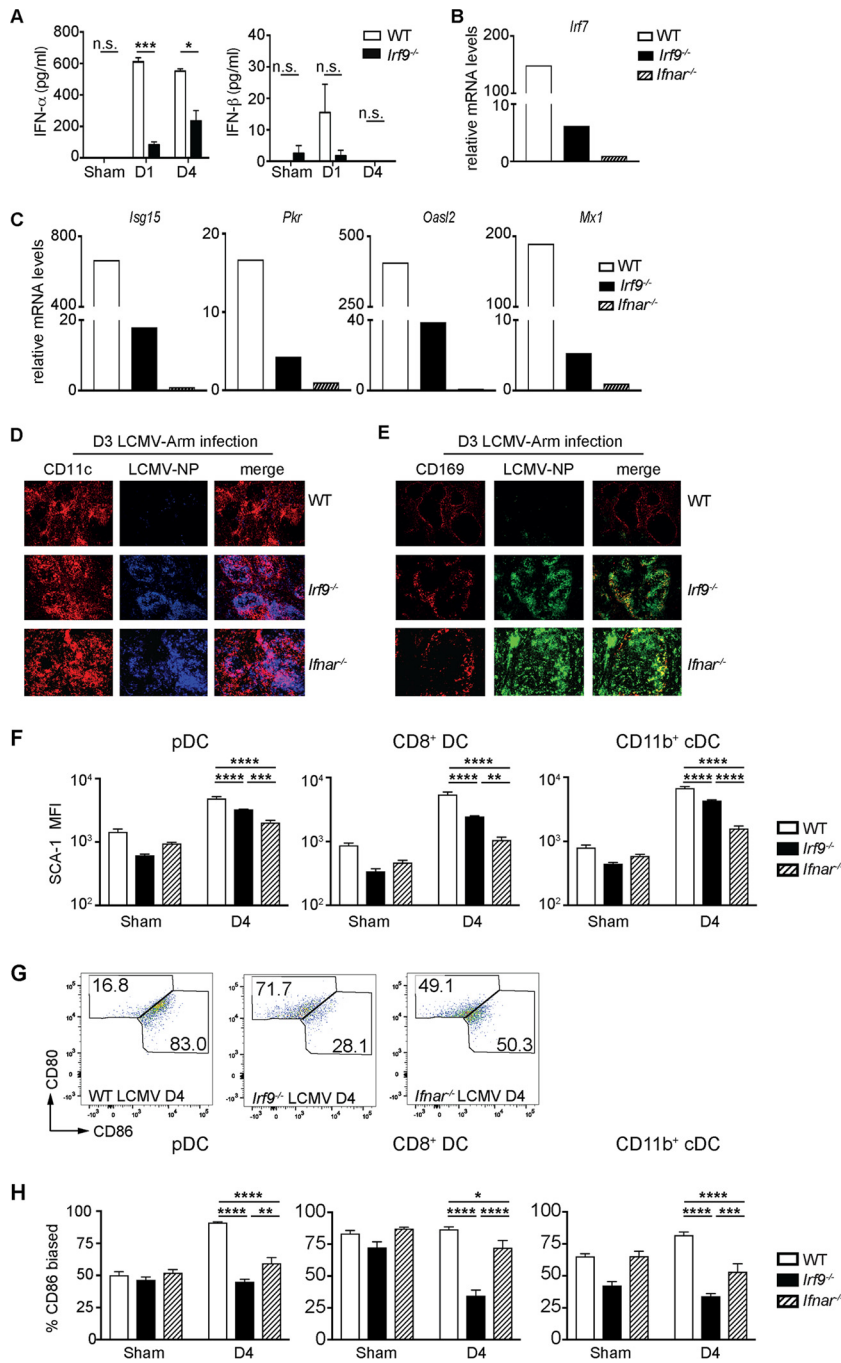
FIG 6 IRF9 is essential for dendritic cell function and early restriction of LCMV-Arm dissemination. (A to H) WT, $Irf9^{-/-}$, and $Ifnar^{-/-}$ mice were infected with LCMV-Arm and analyzed at the indicated time points p.i. (A) IFN-α and IFN-β levels in plasma at the indicated time points p.i. ($n = 4$ per group). (B and C) Enriched pDCs of WT, $Irf9^{-/-}$, and $Ifnar^{-/-}$ mice at day 1 p.i. were used for RNA isolation and qRT-PCR analysis. The values were normalized to the levels of the 18S rRNA gene, and relative expression was calculated by setting the value for $Ifnar^{-/-}$ mice to 1. (D and E) Immunofluorescence of spleen sections from WT, $Irf9^{-/-}$, and $Ifnar^{-/-}$ mice at day 3 p.i., stained for LCMV-NP, CD11c (DCs), and CD169 (metallophilic macrophages adjacent to the marginal zone of the spleen) ($n = 3$ per group). Original magnification, ×10. (F to H) *Ex vivo* flow analysis of SCA-1, CD80, and CD86 on pDCs (CD3e⁻ NK1.1⁻ B220⁺ CD11c⁺), CD8⁺ cDCs (CD3e⁻ NK1.1⁻ B220⁻ CD11cʰⁱ MHCʰⁱ CD8a⁺), and CD11b⁺ cDCs (CD3e⁻ NK1.1⁻ B220⁻ CD11cʰⁱ MHCʰⁱ CD11b⁺) at day 4 p.i. *, $P < 0.05$; **, $P < 0.01$; ***, $P < 0.001$; ****, $P < 0.0001$; n.s., not significant (unpaired two-tailed Student's *t* test).

IRF9-dependent IFN-I signaling is critical for the early control of LCMV replication, a crucial event in the establishment of infection (2, 3, 29).

The impaired upregulation of antiviral effectors in LCMV-Arm-infected *Irf9*$^{-/-}$ mice was accompanied by significantly reduced systemic levels of IFN-α and, to a lesser extent, IFN-β. Recently, it was suggested that IFN-α rather than IFN-β is primarily responsible for the early antiviral activity of IFN-I (32). It is likely that the combination of IRF9-dependent effects on IFN-α production and expression of antiviral effectors is critical for limiting early LCMV-Arm replication. This is supported by findings in *Irf7*$^{-/-}$ mice where reduced systemic levels of IFN-α but normal IFN-β levels coincided with increased early LCMV-Arm replication (19, 20). Considering that IRF9 is expressed in most cell types (8) and IFN-β can be produced by almost every cell (29), it is probable that stromal cells also contribute to IRF9-dependent restriction of viral replication and IFN-β production. In addition to restricting viral replication, IFN-I promote the expansion and activation of antiviral CD8$^+$ T cells by substituting for CD4$^+$ T cell help (3, 33–35), inhibiting regulatory T cells (36), and preventing NK cell-mediated cytotoxicity (37, 38). Furthermore, retained IFN-α production during early infection plays an important role in preventing CD8$^+$ T cell exhaustion (39). In this context, our data indicate that CD8$^+$ T cell intrinsic IRF9 appears not to contribute to the promotion of proliferation and activation of CD8$^+$ T cells, known as signal 3, provided by cytokines (3). Note that recent studies have shown that in contrast to the early antiviral response, where IFN-I are required for virus control and elimination, prolonged IFN-I responses during chronic infection contribute to CD8$^+$ T cell exhaustion (40, 41).

Strikingly, the prevention of CD8$^+$ T cell exhaustion was mediated in a manner extrinsic to CD8$^+$ T cells through multiple IRF9- and IFNAR-dependent effects. Antigen overstimulation induces CD8$^+$ T cell exhaustion (3, 42–44). IRF9-dependent early control of virus dissemination in concert with increased IFN-I action potentially promotes CD8$^+$ T cell activity and operates as the main mechanism by which IRF9 downstream of IFNAR prevents CD8$^+$ T cell exhaustion. Moreover, IRF9 affected the balance of expression of the costimulatory molecules CD80 and CD86 on pDCs and cDCs. Since appropriate costimulatory signals are important for optimal DC-mediated CD8$^+$ T cell activation (2), it is possible that this imbalance further contributed to the induction of CD8$^+$ T cell exhaustion in the *Irf9*$^{-/-}$ mice. Thus, the exhaustion of the CD8$^+$ T cell response and subsequent LCMV persistence that were caused by IRF9 or IFNAR deficiency were probably triggered by a combination of factors, including loss of restriction of viral replication, impaired IFN-I production, and defects in DCs.

The contribution of pDCs to the immune response against LCMV is a matter of ongoing discussion. However, it has been reported that pDCs are productively infected and activated via TLR7 during infection with LCMV and other arenaviruses, such as Lassa virus (45). A role for pDCs in the host response against LCMV also comes from findings from mice with Runx2-deficient pDCs (46). Runx2-deficient pDCs produce less IFN-α following LCMV infection, resulting in an impaired antiviral CD8$^+$ T cell response that is characterized by the expression of PD1 and impaired clearance of acute infection with an LCMV strain. The similarities between that study (46) and the results reported here suggest that the effects of IRF9 in pDCs and CD8$^+$ and CD11b$^+$ cDCs are critical for a normal host response. Consequently, IRF9 deficiency in DCs contributed directly to the phenotype of *Irf9*$^{-/-}$ mice infected with LCMV-Arm. This is supported by our results, obtained from Flt3L-DCs, showing a fundamental role of IRF9 in DCs for IFN-I-mediated upregulation of IFN-I, antiviral effectors, and the TF IRF7. Note that the genes for IRF9, IRF7, and many antiviral effectors are themselves ISGs with interferon-stimulated response elements (ISREs) in their promoters (12, 13, 29), which act as binding sites for the ISGF3 complex (47). Therefore, it is conceivable that their expression is directly regulated by the ISGF3 complex.

The specific function of IRF9 in coordinating the IFN-I response against LCMV is underscored by differences in clinical phenotype between *Irf9*$^{-/-}$, *Ifnar*$^{-/-}$, and *Stat1*$^{-/-}$ mice. While infection of *Stat1*$^{-/-}$ mice with LCMV results in a lethal wasting disease that is mediated by CD4$^+$ T cells (18), *Ifnar*$^{-/-}$ and *Irf9*$^{-/-}$ mice survive and

develop LCMV persistence (19), suggesting that IRF9 is an essential facilitator of effects mediated via IFNAR during LCMV infection. The differences in clinical severity between $Irf9^{-/-}$ and $Ifnar^{-/-}$ mice are likely the consequence of aberrant IFN-I signaling in the former. We previously showed that in the absence of IRF9, IFN-I induce an IFN-γ-like response (48). In support of this, mRNA levels for a number of proinflammatory genes, including *Cxcl9* and *Irf1*, were increased in the CNS of infected $Irf9^{-/-}$ mice compared to those in the CNS of $Ifnar^{-/-}$ mice (data not shown). Thus, alternative IRF9-independent IFN-I signaling may account for the increased disease severity in IRF9-deficient mice. Furthermore, the levels of antiviral effectors and the IFN-I-inducible marker SCA-1 were affected more strongly in DCs isolated from IFNAR-deficient mice than in those from IRF9-deficient mice compared to the levels in WT mice, indicating a contribution of alternative IRF9-independent pathways downstream of IFNAR signaling to the control of early responses to LCMV. Finally, the expression of costimulatory molecules was differentially regulated in IFNAR- and IRF9-deficient DCs, suggesting unequal regulation of these molecules by IFNAR and IRF9 signaling and a slight variability in the CD8$^+$ T cell response. Nevertheless, our findings illustrate a pivotal role of the IRF9 signaling pathway downstream of IFNAR in determining the course of LCMV infection by preventing CD8$^+$ T cell exhaustion in an extrinsic manner. Thus, the extent of IRF9 expression might be used in the future as a predictive marker for the detection of the course of the immune response and the outcome of infection.

MATERIALS AND METHODS

Mice. $Irf9^{-/-}$, $Ifnar^{-/-}$, and P14 mice were described previously (11, 21, 22). Wild-type (WT) C57BL/6 and congenic CD45.1 (Ly5.1) (6.SJL-*Ptprc^a Pep3^b*/BoyJ) mice were purchased from The Jackson Laboratory. WT P14 mice were kindly provided by Max Loehning, German Rheumatism Research Center Berlin. P14 mice were bred with $Irf9^{-/-}$ mice to generate $Irf9^{-/-}$ P14 mice. All mice were on a C57BL/6 genetic background and were bred under specific-pathogen-free conditions at the animal facility of the Biomedical Research Center, University Marburg, or at the animal facility of the University of Sydney. Ethics approval for all animal experiments was obtained from the animal ethics committees of The University of Sydney (approval no. 5883/2013 and 1056/2016) and the Regierungspraesidium Giessen (approval no. 53-2010). Animal experiments were performed in compliance with the NSW Animal Research Act (and its associated regulations) and the 2004 NHMRC Australian code of practice for the care and use of animals for scientific purposes, for experiments performed in Australia, or in compliance with the German animal protection law (TierSchG), for animal experiments performed in Germany.

Preparation of LCMV stock and infection of mice. LCMV-Arm was kindly provided by Peter Aichele, University of Freiburg. Virus was propagated in Vero cells (kindly provided by Markus Eickmann), and infectivity was determined by a plaque formation assay as previously described (18). For infections, mice between 8 and 16 weeks of age were used. For experiments with T cell transfers and T cell responses, mice were injected with 2×10^5 PFU LCMV-Arm i.p., and for the clinical course and histology experiments shown in Fig. 1, the mice were injected with 10^3 PFU LCMV-Arm i.p. Following infection, mice were weighed and observed daily for the development of signs of disease. Clinical scores were determined by adding up individual scores based on an animal ethics committee-approved scoring scheme (rough fur = 1, prominent vertebral spinous processes, scapulae, or pelvis = 2, hunched posture = 2, reduced activity = 2, tremor = 3, and seizures = 4).

Histology. To determine pathological changes, mice were euthanized at the times shown, and the brains and organs (lungs, liver, spleen, and kidneys) were removed and fixed overnight in ice-cold 4% formaldehyde in phosphate-buffered saline (PBS; pH 7.4). Following paraffin embedding, tissue sections (5 μm) were prepared and stained with hematoxylin and eosin (H&E). For immunofluorescence assay, snap-frozen spleens were analyzed with a monoclonal antibody (MAb) to LCMV-NP (VL4). DCs were stained with anti-CD11c (N418; eBioscience), and macrophages were stained with anti-mSiglec-1 (CD169; R&D Systems).

Plasma isolation and ELISA. Blood was collected from anesthetized mice by cardiac puncture, using a 1-ml syringe containing 20 μl heparin (10 kU/ml; Sigma-Aldrich, Castle Hill, Australia). Blood was centrifuged for 5 min at 2,000 $\times$ g at 4°C, and the supernatant was removed, placed in aliquots, snap-frozen in liquid nitrogen, and stored at -80°C. Enzyme-linked immunosorbent assays (ELISAs) for IFN-α (PBL Biomedical Laboratories, NJ, USA) and IFN-β (MyBioSource, CA, USA) were done according to the manufacturers' instructions.

Isolation and transfer of cells and flow cytometry. Splenocytes in single-cell suspension were stained for cell surface markers by use of specific antibodies, as indicated. LCMV-specific CD8$^+$ T cells were detected with H-2D^{b}GP$_{33-41}$ or H-2D^{b}NP$_{396-404}$ dextramers (Immudex, Copenhagen, Denmark), followed by extracellular staining with the indicated fluorochrome-conjugated antibodies. For the characterization of cytokine production, cells were incubated with 1 μM LCMV GP$_{33-41}$ (KAVYNFATM) or 1 μM NP$_{396-404}$ (FQPQNGQFI) in the presence of brefeldin A (Sigma-Aldrich, St. Louis, USA) for 4 h. Cells were stained for CD8α, fixed with 2% formalin, permeabilized with 0.1% saponin, and stained for TNF-α and IFN-γ. Fluorochrome-conjugated antibodies used were anti-CD8α (53-6.7; BD Pharmingen or Bio-

Legend), anti-CD44 (IM7; BD Pharmingen or BioLegend), anti-KLRG1 (2F1; eBioscience or BioLegend), anti-LAG3 (C9B7W; BD Pharmingen or BioLegend), anti-PD1 (J43 [eBioscience] or 29F.1A12 [BioLegend]), anti-CD4 (RM4-5; BD Biosciences or BioLegend), anti-CD3e (145-2C11; BioLegend or BD Pharmingen), anti-CD45 (30-F11; BioLegend), anti-TNF-α (MAb11; eBioscience), and anti-IFN-γ (XMG1.2; BioLegend). For intranuclear staining, anti-T-bet (eBio4B10; eBioscience) and anti-Eomes (Dan11mag; eBioscience) MAbs were used. For transfers, CD8$^+$ T cells were purified from single-cell splenocyte suspensions by use of a kit for negative selection of CD8$^+$ T cells (Miltenyi) following the manufacturer's instructions. The transferred cells were detected by surface staining with anti-CD45.2 (104; Biolegend) or anti-CD45.1 (A20; BD Pharmingen). For experiments characterizing P14 responses, 10^4 P14 or $Irf9^{-/-}$ P14 cells were transferred i.p. Cells from spleens were analyzed with a FACSCanto II or Aria III flow cytometer and FlowJo software.

qRT-PCR and RPA. For qRT-PCR, total RNA was prepared using an RNeasy microkit (Qiagen, Hilden, Germany). cDNA synthesis and PCR were performed as described previously (49). mRNA levels were normalized to 18S or HPRT1 mRNA levels by use of the $\Delta\Delta C_T$ method, and relative fold differences were calculated. Previously published primer sequences for detection of mouse $Irf7$, $Isg15$, $Mx1$, Pkr, and $Oasl2$ (50) were used. For RNase protection assay (RPA), RNA was isolated using TRIsure (Bioline, Alexandria, NSW, Australia). RPA against LCMV-NP was performed as previously described (18).

Generation and stimulation of Flt3L-DCs and ELISA. For the generation of Flt3L-induced DC cultures, murine BM cells were seeded at 1.5×10^6 cells/ml in medium supplemented with Flt3L-containing cell supernatant (1:250) for 7 days, as described previously (51). For in $vitro$ stimulation, Flt3L-DCs were stimulated with 1 μg/ml LPS (Sigma-Aldrich), 0.75 μM RNA40 (IBA, Göttingen, Germany), 1 μM CpG-ODN2216 (CpG2216; TIB Molbiol, Berlin, Germany), or 2,500 U/ml murine IFN-β (Chemicon, PBL). RNA40 was complexed with N-[1-(2,3-dioleoyloxy)propyl]-N,N,N-trimethylammonium methyl-sulfate (DOTAP; Carl Roth, Karlsruhe, Germany) according to the manufacturer's instructions. Supernatants were collected after 22 h of stimulation and analyzed for IL-6, IL-12p40, and TNF-α by use of ELISA kits (all from BD Biosciences) according to the manufacturer's instructions. Concentrations of mouse IFN-α and IFN-β were analyzed using specific capture and detection antibodies (PBL Assay Science).

Immunoblotting. Flt3L-DCs from WT and $Irf9^{-/-}$ mice were harvested after 7 days of differentiation with Flt3L, washed with PBS, seeded in a 24-well plate at 10^6 cells/well, and incubated for 22 h in the presence of RNA40 or CpG2216. Cells were then collected and lysed using RIPA buffer (Sigma-Aldrich). The lysates were fractioned by SDS-PAGE, transferred to a polyvinylidene difluoride (PVDF) membrane, and immunoblotted as described previously (49) and then were stained with rabbit monoclonal antibodies against IRF7 (EPR4718; Abcam), p44/42 mitogen-activated protein kinases (MAPK) (4696; Cell Signaling), NF-κB p65 (C20; Santa Cruz Biotechnology), and β-actin (AC-15; Sigma-Aldrich).

***Ex vivo* purification and staining of pDCs.** Spleens from day 1 p.i. with LCMV-Arm (2×10^5 PFU) from WT or $Irf9^{-/-}$ mice (pooled from 6 mice per group) were processed for pDC purification by use of a negative selection kit (Miltenyi) according to the manufacturer's instructions. Thereafter, the cells were stained in the presence of anti-CD16/CD32 antibodies (93; eBioscience) for surface expression of Siglec-H and B220 for characterization of pDCs. For ex $vivo$ DC analysis, 2×10^6 splenocytes/well were stained with fixable blue LIVE/DEAD reagent (1/1,000; Life Technologies) and purified with anti-mouse CD16/32 (1/100) in PBS for 20 min at 4°C before adding anti-CD11b (M1/70; BD Biosciences), anti-CD11c (N418; BioLegend), anti-Siglec-F (E50-2440; BD Biosciences), anti-I-A/I-E (M5/114.15.2; BioLegend), anti-NK1.1 (PK135; BioLegend), anti-CD45 (30-F11; BD Biosciences), anti-CD8a (53-6.7; BioLegend), anti-B220 (RA3-6B2; BioLegend), anti-I-Ab (AF6-120.1; BioLegend), anti-CD317 (anti-PDCA-1 or -tetherin) (297; BioLegend), anti-CD80 (16-10A1; BD Biosciences), anti-CD3e (145-2C11; BioLegend), anti-CD274 (anti-PDL1 or -B7-H1) (10G.9G2; BioLegend), anti-Ly6C (HK1.4; BioLegend), anti-Ly6G (1A8; BioLegend), or anti-CD86 (GL-1; BioLegend). Cells were incubated for a further 30 min at 4°C before centrifugation. Samples were washed twice, fixed in fixation buffer (BioLegend) for 10 min, washed, and resuspended in fluorescence-activated cell sorter (FACS) buffer.

Statistics. All described experiments were performed at least twice with similar results, unless otherwise indicated. Details of statistical analysis are given in the figure legends.

REFERENCES

1. Kaech SM, Cui W. 2012. Transcriptional control of effector and memory CD8(+) T cell differentiation. Nat Rev Immunol 12:749–761. https://doi.org/10.1038/nri3307.

2. Wherry EJ, Kurachi M. 2015. Molecular and cellular insights into T cell exhaustion. Nat Rev Immunol 15:486–499. https://doi.org/10.1038/nri3862.

3. Crouse J, Kalinke U, Oxenius A. 2015. Regulation of antiviral T cell responses by type I interferons. Nat Rev Immunol 15:231–242. https://doi.org/10.1038/nri3806.

4. Wherry EJ. 2011. T cell exhaustion. Nat Immunol 12:492–499. https://doi.org/10.1038/ni.2035.

5. Speiser DE, Utzschneider DT, Oberle SG, Munz C, Romero P, Zehn D. 2014. T cell differentiation in chronic infection and cancer: functional adaptation or exhaustion? Nat Rev Immunol 14:768–774. https://doi.org/10.1038/nri3740.

6. McNab F, Mayer-Barber K, Sher A, Wack A, O'Garra A. 2015. Type I interferons in infectious disease. Nat Rev Immunol 15:87–103. https://doi.org/10.1038/nri3787.

7. Ivashkiv LB, Donlin LT. 2014. Regulation of type I interferon responses. Nat Rev Immunol 14:36–49. https://doi.org/10.1038/nri3581.

8. Suprunenko T, Hofer MJ. 2016. The emerging role of interferon regulatory factor 9 in the antiviral host response and beyond. Cytokine Growth Factor Rev 29:35–43. https://doi.org/10.1016/j.cytogfr.2016.03.002.

9. Kawakami T, Matsumoto M, Sato M, Harada H, Taniguchi T, Kitagawa M. 1995. Possible involvement of the transcription factor ISGF3 gamma in virus-induced expression of the IFN-beta gene. FEBS Lett 358:225–229. https://doi.org/10.1016/0014-5793(94)01426-2.

10. Harada H, Matsumoto M, Sato M, Kashiwazaki Y, Kimura T, Kitagawa M, Yokochi T, Tan RS, Takasugi T, Kadokawa Y, Schindler C, Schreiber RD, Noguchi S, Taniguchi T. 1996. Regulation of IFN-alpha/beta genes: evidence for a dual function of the transcription factor complex ISGF3 in the production and action of IFN-alpha/beta. Genes Cells 1:995–1005. https://doi.org/10.1046/j.1365-2443.1996.870287.x.

11. Kimura T, Kadokawa Y, Harada H, Matsumoto M, Sato M, Kashiwazaki Y, Tarutani M, Tan RS, Takasugi T, Matsuyama T, Mak TW, Noguchi S, Taniguchi T. 1996. Essential and non-redundant roles of p48 (ISGF3 gamma) and IRF-1 in both type I and type II interferon responses, as revealed by gene targeting studies. Genes Cells 1:115–124. https://doi.org/10.1046/j.1365-2443.1996.08008.x.

12. Kessler DS, Levy DE, Darnell JE, Jr. 1988. Two interferon-induced nuclear factors bind a single promoter element in interferon-stimulated genes. Proc Natl Acad Sci U S A 85:8521–8525. https://doi.org/10.1073/pnas.85.22.8521.

13. Levy DE, Kessler DS, Pine R, Darnell JE, Jr. 1989. Cytoplasmic activation of ISGF3, the positive regulator of interferon-alpha-stimulated transcription, reconstituted in vitro. Genes Dev 3:1362–1371. https://doi.org/10.1101/gad.3.9.1362.

14. Lu R, Au WC, Yeow WS, Hageman N, Pitha PM. 2000. Regulation of the promoter activity of interferon regulatory factor-7 gene. Activation by interferon and silencing by hypermethylation. J Biol Chem 275:31805–31812.

15. Sato M, Hata N, Asagiri M, Nakaya T, Taniguchi T, Tanaka N. 1998. Positive feedback regulation of type I IFN genes by the IFN-inducible transcription factor IRF-7. FEBS Lett 441:106–110. https://doi.org/10.1016/S0014-5793(98)01514-2.

16. Gilliet M, Cao W, Liu YJ. 2008. Plasmacytoid dendritic cells: sensing nucleic acids in viral infection and autoimmune diseases. Nat Rev Immunol 8:594–606. https://doi.org/10.1038/nri2358.

17. Honda K, Yanai H, Negishi H, Asagiri M, Sato M, Mizutani T, Shimada N, Ohba Y, Takaoka A, Yoshida N, Taniguchi T. 2005. IRF-7 is the master regulator of type-I interferon-dependent immune responses. Nature 434:772–777. https://doi.org/10.1038/nature03464.

18. Hofer MJ, Li W, Manders P, Terry R, Lim SL, King NJ, Campbell IL. 2012. Mice deficient in STAT1 but not STAT2 or IRF9 develop a lethal CD4+ T-cell-mediated disease following infection with lymphocytic choriomeningitis virus. J Virol 86:6932–6946. https://doi.org/10.1128/JVI.07147-11.

19. Li W, Hofer MJ, Jung SR, Lim SL, Campbell IL. 2014. IRF7-dependent type I interferon production induces lethal immune-mediated disease in STAT1 knockout mice infected with lymphocytic choriomeningitis virus. J Virol 88:7578–7588. https://doi.org/10.1128/JVI.03117-13.

20. Zhou S, Cerny AM, Fitzgerald KA, Kurt-Jones EA, Finberg RW. 2012. Role of interferon regulatory factor 7 in T cell responses during acute lymphocytic choriomeningitis virus infection. J Virol 86:11254–11265. https://doi.org/10.1128/JVI.00576-12.

21. Muller U, Steinhoff U, Reis LF, Hemmi S, Pavlovic J, Zinkernagel RM, Aguet M. 1994. Functional role of type I and type II interferons in antiviral defense. Science 264:1918–1921. https://doi.org/10.1126/science.8009221.

22. Pircher H, Burki K, Lang R, Hengartner H, Zinkernagel RM. 1989. Tolerance induction in double specific T-cell receptor transgenic mice varies with antigen. Nature 342:559–561. https://doi.org/10.1038/342559a0.

23. Probst HC, van den Broek M. 2005. Priming of CTLs by lymphocytic choriomeningitis virus depends on dendritic cells. J Immunol 174:3920–3924. https://doi.org/10.4049/jimmunol.174.7.3920.

24. Sevilla N, Kunz S, Holz A, Lewicki H, Homann D, Yamada H, Campbell KP, de La Torre JC, Oldstone MB. 2000. Immunosuppression and resultant viral persistence by specific viral targeting of dendritic cells. J Exp Med 192:1249–1260. https://doi.org/10.1084/jem.192.9.1249.

25. Homann D, McGavern DB, Oldstone MB. 2004. Visualizing the viral burden: phenotypic and functional alterations of T cells and APCs during persistent infection. J Immunol 172:6239–6250. https://doi.org/10.4049/jimmunol.172.10.6239.

26. Cao W, Henry MD, Borrow P, Yamada H, Elder JH, Ravkov EV, Nichol ST, Compans RW, Campbell KP, Oldstone MB. 1998. Identification of alpha-dystroglycan as a receptor for lymphocytic choriomeningitis virus and Lassa fever virus. Science 282:2079–2081. https://doi.org/10.1126/science.282.5396.2079.

27. Naik SH, Sathe P, Park HY, Metcalf D, Proietto AI, Dakic A, Carotta S, O'Keeffe M, Bahlo M, Papenfuss A, Kwak JY, Wu L, Shortman K. 2007. Development of plasmacytoid and conventional dendritic cell subtypes from single precursor cells derived in vitro and in vivo. Nat Immunol 8:1217–1226. https://doi.org/10.1038/ni1522.

28. Siegfried A, Berchtold S, Manncke B, Deuschle E, Reber J, Ott T, Weber M, Kalinke U, Hofer MJ, Hatesuer B, Schughart K, Gailus-Durner V, Fuchs H, Hrabe de Angelis M, Weber F, Hornef MW, Autenrieth IB, Bohn E. 2013. IFIT2 is an effector protein of type I IFN-mediated amplification of lipopolysaccharide (LPS)-induced TNF-alpha secretion and LPS-induced endotoxin shock. J Immunol 191:3913–3921. https://doi.org/10.4049/jimmunol.1203305.

29. Schneider WM, Chevillotte MD, Rice CM. 2014. Interferon-stimulated genes: a complex web of host defenses. Annu Rev Immunol 32:513–545. https://doi.org/10.1146/annurev-immunol-032713-120231.

30. Niederquell M, Kurig S, Fischer JA, Tomiuk S, Swiecki M, Colonna M, Johnston IC, Dzionek A. 2013. Sca-1 expression defines developmental stages of mouse pDCs that show functional heterogeneity in the endosomal but not lysosomal TLR9 response. Eur J Immunol 43:2993–3005. https://doi.org/10.1002/eji.201343498.

31. Schlitzer A, McGovern N, Ginhoux F. 2015. Dendritic cells and monocyte-derived cells: two complementary and integrated functional systems. Semin Cell Dev Biol 41:9–22. https://doi.org/10.1016/j.semcdb.2015.03.011.

32. Ng CT, Sullivan BM, Teijaro JR, Lee AM, Welch M, Rice S, Sheehan KC, Schreiber RD, Oldstone MB. 2015. Blockade of interferon beta, but not interferon alpha, signaling controls persistent viral infection. Cell Host Microbe 17:653–661. https://doi.org/10.1016/j.chom.2015.04.005.

33. Wiesel M, Crouse J, Bedenikovic G, Sutherland A, Joller N, Oxenius A. 2012. Type-I IFN drives the differentiation of short-lived effector CD8+ T cells in vivo. Eur J Immunol 42:320–329. https://doi.org/10.1002/eji.201142091.

34. Aichele P, Unsoeld H, Koschella M, Schweier O, Kalinke U, Vucikuja S. 2006. CD8 T cells specific for lymphocytic choriomeningitis virus require type I IFN receptor for clonal expansion. J Immunol 176:4525–4529. https://doi.org/10.4049/jimmunol.176.8.4525.

35. Kolumam GA, Thomas S, Thompson LJ, Sprent J, Murali-Krishna K. 2005. Type I interferons act directly on CD8 T cells to allow clonal expansion and memory formation in response to viral infection. J Exp Med 202:637–650. https://doi.org/10.1084/jem.20050821.

36. Srivastava S, Koch MA, Pepper M, Campbell DJ. 2014. Type I interferons directly inhibit regulatory T cells to allow optimal antiviral T cell responses during acute LCMV infection. J Exp Med 211:961–974. https://doi.org/10.1084/jem.20131556.

37. Xu HC, Grusdat M, Pandyra AA, Polz R, Huang J, Sharma P, Deenen R, Kohrer K, Rahbar R, Diefenbach A, Gibbert K, Lohning M, Hocker L, Waibler Z, Haussinger D, Mak TW, Ohashi PS, Lang KS, Lang PA. 2014. Type I interferon protects antiviral CD8+ T cells from NK cell cytotoxicity. Immunity 40:949–960. https://doi.org/10.1016/j.immuni.2014.05.004.

38. Crouse J, Bedenikovic G, Wiesel M, Ibberson M, Xenarios I, Von Laer D, Kalinke U, Vivier E, Jonjic S, Oxenius A. 2014. Type I interferons protect T cells against NK cell attack mediated by the activating receptor NCR1. Immunity 40:961–973. https://doi.org/10.1016/j.immuni.2014.05.003.

39. Wang Y, Swiecki M, Cella M, Alber G, Schreiber RD, Gilfillan S, Colonna M. 2012. Timing and magnitude of type I interferon responses by distinct sensors impact CD8 T cell exhaustion and chronic viral infection. Cell Host Microbe 11:631–642. https://doi.org/10.1016/j.chom.2012.05.003.

40. Teijaro JR, Ng C, Lee AM, Sullivan BM, Sheehan KC, Welch M, Schreiber

RD, de la Torre JC, Oldstone MB. 2013. Persistent LCMV infection is controlled by blockade of type I interferon signaling. Science 340: 207–211. https://doi.org/10.1126/science.1235214.

41. Wilson EB, Yamada DH, Elsaesser H, Herskovitz J, Deng J, Cheng G, Aronow BJ, Karp CL, Brooks DG. 2013. Blockade of chronic type I interferon signaling to control persistent LCMV infection. Science 340: 202–207. https://doi.org/10.1126/science.1235208.

42. Moskophidis D, Lechner F, Pircher H, Zinkernagel RM. 1993. Virus persistence in acutely infected immunocompetent mice by exhaustion of antiviral cytotoxic effector T cells. Nature 362:758–761. https://doi.org/10.1038/362758a0.

43. Zajac AJ, Blattman JN, Murali-Krishna K, Sourdive DJ, Suresh M, Altman JD, Ahmed R. 1998. Viral immune evasion due to persistence of activated T cells without effector function. J Exp Med 188:2205–2213. https://doi.org/10.1084/jem.188.12.2205.

44. Gallimore A, Glithero A, Godkin A, Tissot AC, Pluckthun A, Elliott T, Hengartner H, Zinkernagel R. 1998. Induction and exhaustion of lymphocytic choriomeningitis virus-specific cytotoxic T lymphocytes visualized using soluble tetrameric major histocompatibility complex class I-peptide complexes. J Exp Med 187:1383–1393. https://doi.org/10.1084/jem.187.9.1383.

45. Macal M, Lewis GM, Kunz S, Flavell R, Harker JA, Zuniga EI. 2012. Plasmacytoid dendritic cells are productively infected and activated through TLR-7 early after arenavirus infection. Cell Host Microbe 11: 617–630. https://doi.org/10.1016/j.chom.2012.04.017.

46. Chopin M, Preston SP, Lun AT, Tellier J, Smyth GK, Pellegrini M, Belz GT, Corcoran LM, Visvader JE, Wu L, Nutt SL. 2016. RUNX2 mediates plasmacytoid dendritic cell egress from the bone marrow and controls viral immunity. Cell Rep 2016:S2211-1247(16)30355-2. https://doi.org/10.1016/j.celrep.2016.03.066.

47. Huber M, Lohoff M. 2014. IRF4 at the crossroads of effector T-cell fate decision. Eur J Immunol 44:1886–1895. https://doi.org/10.1002/eji.201344279.

48. Hofer MJ, Li W, Lim SL, Campbell IL. 2010. The type I interferon-alpha mediates a more severe neurological disease in the absence of the canonical signaling molecule interferon regulatory factor 9. J Neurosci 30:1149–1157. https://doi.org/10.1523/JNEUROSCI.3711-09.2010.

49. Raczkowski F, Ritter J, Heesch K, Schumacher V, Guralnik A, Hocker L, Raifer H, Klein M, Bopp T, Harb H, Kesper DA, Pfefferle PI, Grusdat M, Lang PA, Mittrucker HW, Huber M. 2013. The transcription factor interferon regulatory factor 4 is required for the generation of protective effector CD8+ T cells. Proc Natl Acad Sci U S A 110:15019–15024. https://doi.org/10.1073/pnas.1309378110.

50. Hernandez PP, Mahlakoiv T, Yang I, Schwierzeck V, Nguyen N, Guendel F, Gronke K, Ryffel B, Holscher C, Dumoutier L, Renauld JC, Suerbaum S, Staeheli P, Diefenbach A. 2015. Interferon-lambda and interleukin 22 act synergistically for the induction of interferon-stimulated genes and control of rotavirus infection. Nat Immunol 16:698–707. https://doi.org/10.1038/ni.3180.

51. Yu P, Lubben W, Slomka H, Gebler J, Konert M, Cai C, Neubrandt L, Prazeres da Costa O, Paul S, Dehnert S, Dohne K, Thanisch M, Storsberg S, Wiegand L, Kaufmann A, Nain M, Quintanilla-Martinez L, Bettio S, Schnierle B, Kolesnikova L, Becker S, Schnare M, Bauer S. 2012. Nucleic acid-sensing Toll-like receptors are essential for the control of endogenous retrovirus viremia and ERV-induced tumors. Immunity 37:867–879. https://doi.org/10.1016/j.immuni.2012.07.018.